Revista Cubana de Química. Vol.37.2025(26-39)
https://cubanadequimica.uo.edu.cu/index.php/cq
Research Papers

ALGINATE-LIGNIN AND ALGINATE-SILICA MICROCAPSULES CONTAINING GRAPEFRUIT ESSENTIAL OIL AND THEIR CONTROLLED RELEASE MODELLING

MICROENCAPSULACIÓN DE ACEITE ESENCIAL DE POMELO EN MATRICES DE ALGINATO-LIGNINA Y ALGINATO-SÍLICE Y MODELADO DE SU LIBERACIÓN CONTROLADA

Liliana Mariel-Cáceres[1*], https://orcid.org/0000-0002-2939-1581
Eliana Paola Dagnino[1], https://orcid.org/0000-0002-8560-5484
Ester Chamorro[1], https://orcid.org/0000-0002-6110-4511

[1]Centro de Investigación en Química Orgánica Biológica, Facultad Regional Resistencia, Universidad Tecnológica Nacional (QUIMOBI-FRRE-UTN), Argentina

*Corresponding author: lmarielc@ca.frre.utn.edu.ar; lmarielc@yahoo.com.ar

Recibido: 20 de julio de 2024 Aprobado: 1 de diciembre de 2024

ABSTRACT

The encapsulation methodology protects essential oils from external factors (air, light, moisture, and high temperatures), limits its degradation, and allows its slow release. This study aimed at optimizing the encapsulation by ionic gelation of grapefruit essential oil in sodium alginate matrix obtaining a yield of more than 50 % and having an efficiency of more than 90 %. Two new matrices were studied, combining sodium alginate with lignin and silica. These components were obtained from biomass rice husks and showed an efficiency of 99,91 %, a yield of 67,183 % when having 1 % of lignin concentration and an efficiency rate of 97,67 %, and a yield of 52,306 % with 0,8 % of silica. Furthermore, vacuum drying was used and it significantly reduced the size and moisture of the microcapsules. The profiles of controlled release considered in each case were adjusted to Peppas and Korsmeyer's model for polymeric systems.

Keywords: encapsulation; alginate; lignin; silica; essential oils.

RESUMEN

La metodología de encapsulación protege los aceites esenciales de factores externos (aire, luz, humedad y altas temperaturas), limita su degradación y permite su lenta liberación. Este estudio tuvo como objetivo optimizar la encapsulación por gelificación iónica de aceite esencial de pomelo en matriz de alginato de sodio, obteniendo un rendimiento superior al 50 %, y teniendo una eficiencia superior al 90 %. Se estudiaron dos nuevas matrices que combinan alginato de sodio con lignina y sílice. Estos componentes se obtuvieron a partir de biomasa de cascarilla de arroz y mostraron una eficiencia del 99,91 %, un rendimiento del 67,18 % al tener una concentración de lignina del 1 % y una tasa de eficiencia del 97,67 %, y un rendimiento del 52,31% con 0,8 % de sílice. Además, se utilizó secado al vacío reduciendo el tamaño y la humedad de las microcápsulas. Los perfiles de liberación controlada considerados en cada caso se ajustaron al modelo de Peppas y Korsmeyer para sistemas poliméricos.

Palabras clave: encapsulación; alginato; lignina; sílica; aceites esenciales

INTRODUCTION

At present, essential oils (EOs) have become an integral element of our everyday life as part of a great variety of products (food, cigarettes, cosmetics, perfumes, household aerosols, among others). The antimicrobial potential of these compounds has lately become relevant leading to its study as biocides and as insect repellents.[1] The disadvantage of using EOs is their sensitivity to external factors such as ultraviolet light, high temperatures, and water which affect their composition, making them chemically unstable, and losing their specific properties (scent, antimicrobial activity, flavor, among others).[2] Therefore, it is necessary to develop protection systems such as microencapsulation, which can limit degradation and thus, enable and facilitate their processing and storage[2-4] and their application in small doses.[5]

One of the methodologies of encapsulation easily adaptable to different classes of active principles is the ionic gelation which uses soft process conditions, without high temperatures or solvents and which is a cost-effective process.[6] This technique, coupled with an extrusion, produces spherical microcapsules with drug containment applications, essential oils,[4] and plant extracts.[7] Sodium alginate is one of the most used components for gelation as it is an irreversible hydrocolloid, biocompatible, biodegradable, and inherent in nature.[8-9] The ionic gelation mechanism includes a crosslinking phase, which involves an intermolecular bonding between a divalent cation of the crosslinking substance and the carboxyl groups of sodium alginate.[10] The crosslinking salt concentration (calcium chloride, calcium carbonate, among others) and the crosslinking time affect the encapsulation efficiency and the process yield.[5] The generated matrix can cause a controlled release with a liberation mechanism of the active principle sustained over time.[11]

At the same time, the alginate could also be combined with other polymers, such as chitosan, starch,[12] lignin,[13] and with silica,[14] among others as components of the microcapsules wall to increase yield, efficiency, and controlled release profit from their specific properties.

The aim of this study was to optimize grapefruit essential oil (GEO) encapsulation, which has proven antimicrobial properties[15] in an alginate matrix. To obtain this, the gelation process was optimized (crosslinking concentration and crosslinking time), two new matrices were put forward: alginate-lignin and alginate-silica, and the best proportions of alginate-solid were found, which maximized encapsulation efficiency and yield. The incorporation of essential oils into the matrices was demonstrated through Fourier transform infrared spectrophotometry, UV spectrophotometry, and gas chromatography. Finally, the controlled release of GEO was studied, analyzing adjustments in each case, including experimental data and different mathematical models.

As a result of this study, added value was given not only to grapefruit essential oil, which is a sub-product of a citrus plant of the province of Corrientes, Argentina but also to lignin and silica obtained from husk biorefinery, which is a residue from agricultural businesses of the province of Chaco.

MATERIALS AND METHODS

Materials

Grapefruit essential oil (*Citrus paradisi*) (GEO) which was provided by Mager S.A. from the province of Corrientes, Argentina was used. It is a by-product obtained in the process of grapefruit juice production and it has a density of 0,857 3 ± 0,001 4 mg/m, refractive index of 1,472 3 ± 0,000 3, optical rotation of 91,60 ± 0,11°, and 93 % of limonene as found in previous studies.[15-16] Sodium alginate (Sigma-Aldrich) with an M/G ratio of M/G de 1,56, with 39 % of guluronic acid and 61 % of mannuronic acid and having an amount of 120,000-190,000 g/mol of molecular weight.

The lignin and silica oxide were obtained through the biorefinery process of rice husks. The lignin was extracted sequentially using Organosolv acid containing 1 % inorganic matter and a total of 8,5 % of OH and less than 1 % of sugars.[17] Meanwhile, the silica oxide (silica) was obtained through calcination at 575 °C of the final waste of the biorefinery, deionized water was obtained through reverse osmosis having a 0,2 µS of conductivity at 20 °C, tert-butyl alcohol (p.a. Sintorgan). Isopropyl alcohol (p.a. Sintorgan), 10 mL disposable hypodermic syringe with a metallic needle with 27G beveled edge (0,4 mm x 19 mm).

Raw Material Characterization

To identify the functional groups of GEO, sodium alginate, lignin, and silica, analyses were performed using a Fourier Perkin Elmer-transform infrared absorption spectroscopy with MIRacle ATR base optic accessory and Germanium crystal. The spectra

obtained were compared to those reported in the bibliography and Fluka library supplied by Perkin Elmer. A spectral sweep of diluted GEO in isopropyl alcohol was also made as well as of a sodium alginate solution using a METASH UV-5100-Visible Spectrophotometer, and METASH MetaSpec Pro software.

Preparation of the Alginate-GEO Emulsion

An emulsion with 30 gr of a sodium alginate solution at 1,0 % w/v and the right amount of GEO for a 2 % w/v charge was prepared. It was stirred with a DLAB homogenizer, Model D-500 at 20 000 and 30 000 rpm for 3 min and then it was left standing for an hour to ensure its stability.[12,18]

Microencapsulation and crosslinking optimization

Microcapsules were obtained using the methodology described by other authors with some changes.[5,12] For that purpose, 10 mL of the prepared emulsion was taken with a hypodermic syringe and 27 G needle and placed in an injection pump APEMA model PC11UBT at a preset dropping speed (90 mL/h) from a height of 5 cm over the surface of the solution. These conditions of the encapsulation process were determined in previous studies to obtain spherical capsules smaller than 2 mm.[16]

Droplets fell on the 2,5 and 10 % w/v calcium chloride concentration and then it was allowed to gel keeping a magnetic stirring at 10 rpm for 30, 45, and 60 min consistent with the experimental design which is further detailed. Once crosslinking was finished, capsules were filtered with a steel filter net and then weighed. Afterwards, they were rinsed with alcohol and the liquid was reserved for a further spectrophotometry study. The spectrophotometry results were corroborated by gas chromatography. A Shimadzu GC-14B gas chromatography, Megabore DB-WAX P/N 125-7032 polar column of 30 m x 0,53 mm of internal diameter x 1 µ thickness, connected to a Flame Ionization Detector (FID).

Experimental Design

The optimization of the encapsulation process was carried out through a 3^k statistical, factorial central composite design with k= 2. The selected factors were the concentration of calcium chloride and the cross-linking time (t), each one with three levels, and efficiency and yield as response variables. Two replicas of the design were made of 9 runs each and up to a total of 18 treatments. The results were analysed using Minitab 18 Statistical Software, trial. The mathematic model for the design is the one shown in Equation 1:

$$y = \beta_0 + \sum\beta_i x_i + \sum\beta_{ii} x_{ii}^2 + \sum\beta_{ij} x_i x_j + \varepsilon \quad \textbf{(1)}$$

Where y is the response variable, β_0 is the constant term, β_i are the coefficients of the linear mean effects, β_{ii} are the coefficients of the squared mean effects; β_{ij} are the mean effects of the interactions, x_i and x_j are the independent variables and ε is the random mean error.[19] A variance analysis (ANOVA) was carried out with a significance level of 95 % ($p < 0,05$) maximizing the two response variables. The regression coefficient (R^2) was evaluated: the p-value, the F value of the Fisher test, and the lack of fit to determine the adaptation of the model. Lastly, the model was validated with five runs at the optimal point.

The percentage yield was calculated as the relationship between the mass of the microcapsules obtained and the mass of the raw material used. The percentage yield was calculated with Equation 2.[5]

$$R\,\% = \frac{w_m}{w_a + w_p} 100 \quad (2)$$

where

w_m: mass of the filtered microcapsules.

w_p: mass of the polymer solution (sodium alginate).

w_a: amount of the active principle added to prepare the emulsion.

The percent efficiency of the microcapsules was determined by quantifying the encapsulated GEO. This was calculated by subtracting the surface GEO and the residual GEO in the calcium chloride solution from the initial GEO concentration (w_1). The resulting value (w_2) represents the encapsulated GEO. UV/Vis spectrophotometry at 322 nm with an internal standard was used for all measurements. The Percent Efficiency (E %) was calculated as follows (Equation 3).[8,20]

$$E\% = \frac{w_2}{w_1} 100 \quad (3)$$

Crosslinking Kinetics and Kinetic Model

A 1 % w/v alginate solution, without GEO, was dripped using a syringe pump onto the optimized calcium chloride crosslinking solution. The samples

were allowed to crosslink for periods of 1, 3, 5, 15 and 30 min. The obtained microcapsules were dried in an oven at 100 °C for 12 h and then calcined in a muffle furnace at 750 °C for 8 h until they turned into white ashes. Subsequently, calcium ions were quantified by emission spectroscopy using a Jenway PFP07 (Industrial Version) photometer. The obtained data was fitted to the corresponding model to assess the adsorption kinetics. The Elovich model of general application was used for the chemical absorption processes using Equation 4.[21]

$$\frac{dq_t}{dt} = ae^{-bq_t} \quad (4)$$

where
q_t: amount adsorbed in time t(mg.g^{-1}).
a: initial speed of adsorption (in g.mg^{-1}.min^{-1}).
b: related to the covered surface and the energy of activation by chemical absorption (g.mg^{-1}).

Microcapsules with Modified Matrices

Alginate-Lignin GEO and Alginate-Silica GEO emulsions were prepared by adding these solids at different concentrations (0,5; 0,8 and 1 % w/w) to the original Alginate GEO emulsion. Microencapsulation using these modified matrices was carried out using the previously described optimized methodology. Encapsulation efficiency and yield were evaluated in all cases.

ANOVA with Tukey's post-hoc test was performed to assess mean diffrences. Two comparisons were made: between groups considering the type of solid used as a factor, and another within groups considering the concentration of the solid used as a factor. After filtration, microcapsules with and without solids were dried in an ARCANO vacuum oven at 50 °C, -0,8 Bar, for 60 min.

Characterization of Microcapsules

Moisture

The moisture of microcapsules was determined without GEO in optimized conditions with the different matrices to evaluate the content of water lost during the crosslinking and drying processes. An RADWAG, PMR50 model analytic scale was used to determine the moisture. Measurements were carried out five times.

Size and Morphology

The morphology of microcapsules was analyzed using an optical microscope and a Jeol Modelo 5800 LV electronic microscope (SEM).

The decrease in the size of the microcapsules was analyzed before and after the drying and measuring the diameter of the 10 microcapsules using a LANCET optical microscope with an incorporated digital camera with reduction of the field and ToupCam SCMOS01300KPA software.

Controlled Release

A total of 8 g of wet and dried microcapsules per treatment were dispersed in 60 g of isopropyl alcohol (release medium) and agitated on a flat-orbital shaker (Bioamerican Science Model BS-875) under gentle conditions. Samples were withdrawn at predetermined time intervals and analyzed spectrophotometrically in the UV-Vis region. Cumulative release profiles of GEO were plotted as a function of time, and the data were fitted to various linear models. Regression coefficients were computed to assess the goodness of fit.

RESULTS AND DISCUSSION

Characterization of the Components of the Microcapsules Matrix

The infrared spectrum of GEO (Figure 1a) shows the bending band corresponding to double bonds C=C approximately at 1 600, 1 309, 1 217, 950, 913 and 880 cm^{-1}, the band corresponding to the strain of the bonds =C-H at 3000-3100 cm^{-1} and to -C=C bonds between 1 500 and 1 600 cm^{-1}, similar to what was obtained by other authors.[22] All these groups belong to limonene, which is the major component of the GEO, as well as to myrcene (another terpene component of GEO).

In the sodium alginate spectrum (Figure 1b), the bands related to the OH bonds tension vibration (3250 cm^{-1}), the asymmetric COO- tension vibration (1593 cm^{-1}), the COO symmetric vibration of (close to 1410 cm^{-1}) and the tension band C-O-C and H-O folding at 960-1 100 cm^{-1} are observed.[23]

Besides, the bands between 1 084 y 1 028 cm^{-1}, are due to their saccharide structure, while the bands in the region from 950 to 815 cm^{-1} (948 cm^{-1}, 904 cm^{-1} y 813 cm^{-1}) are associated with acid polyglucuronic

and polymannuronic acids sequences onto the alginate skeleton.[6] The bands of about 948 cm^{-1} are assigned to α 1→4 bond and the bands of 904 cm^{-1} are considered to be the effect of the asymmetric α-L-gulopyranuronic ring.

The lignin spectrum (Figure 1c) exhibits a characteristic band at 3675 cm^{-1}, which is assigned to the stretching vibration of free phenolic hydroxyl groups. The band at 2 968 cm^{-1} is considered the effect of the symmetric vibration of the C-H groups of methylene (-CH2). The bands at 1595 and 1421 cm^{-1} represent the vibration of the aromatic rings. The bands at 1120 and 835 cm^{-1} are assigned to syringyl and guaiacyl units, respectively. The effect of the stretching of the C-OH lateral groups, the C-O-C and glycosidic bonds is observed at 1030 cm^{-1}.

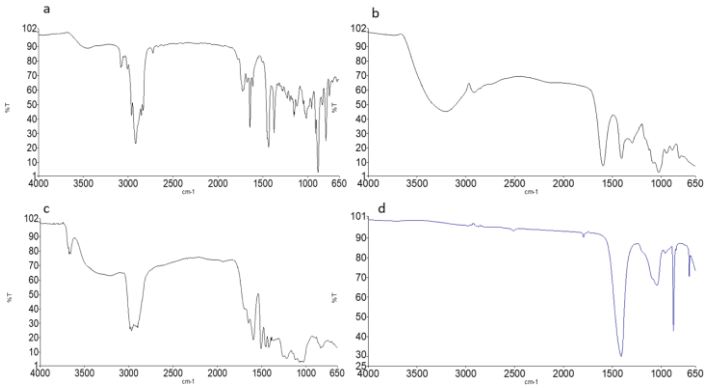

Figure 1- FTIR spectrum, a: grapefruit oil; b: sodium alginate; c: rice husk lignin and d: silica

Besides, the silica spectrum (Figure 1d) visualizes the band at 665 cm^{-1} and registers the SiH_2 mode of flexion. The wideband of 1 020 to 1 100 cm^{-1} is assigned to the tension of the asymmetric mode of the Si-OSi group. Moreover, the Si-CH_2 mode of deformation with a maximum of 1 410 cm^{-1} and the asymmetric stretching of the Si-OSi bond with a maximum of 1 130 cm^{-1} and 1 044 cm^{-1} are observed.[24] Furthermore, a spectral sweep was made in the visible-ultraviolet (of 900 to 200 nm) zone of the GEO observing two bands (232 and 323 nm), which were used to measure its concentration in an alcoholic solution.

Besides, the UV (1090-200 nm) spectral sweep of the sodium alginate shows a maximum peak in the ultraviolet zone at 188 mm corresponding to the carbonyl group.[25]

Alginate- GEO Emulsion

The homogenized emulsion of alginate with 2 % w/w GEO was stable after standing for an hour, without phase separation. Similar results were obtained with analogous concentrations of grapefruit essential oil.[18] Other authors showed stability during the same period with concentrations of palm oil, 5 to 40 % v/v.[12] The droplet formation in the emulsion after it has been homogenized can be observed in Figure 2, with a mean diameter of 0,0011 ± 0,0004 mm, which is less than the diameters obtained by other authors (de 0,0049 a 0,011 mm) with stirring at 10000 rpm with alginate emulsion and limonene oil.[18]

Besides, the asymmetry of the measured diameters was calculated obtaining a value higher than 0.2 which indicates a positive asymmetry; therefore, statistically, samples cannot be represented by their means. The mode of distribution was then calculated (0,0008 mm), which was less than the mean, consistent with its asymmetry. This non-Gaussian distribution is typical of emulsions prepared at high velocity and with very small-sized droplets, which respond to other models of distribution.[26]

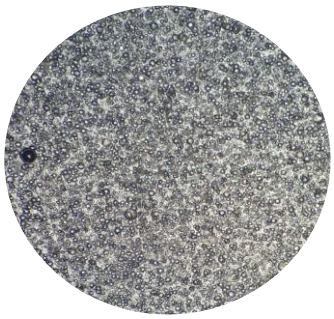

Figure 2- Optical micrograph (10x) of droplets of emulsion: alginate-homogenized grapefruit essential oil at 3 000 rpm

Optimization of Crosslinking

The yields obtained are between 32 and 52 % (data not shown). These low values of yields are due to water loss during the crosslinking process and are confirmed with the analysis of the moisture of the particles after the filtration. This is considered low. Other authors obtained yields between 60,20 % and 62,30 % with a load of thyme essential oil of 3 % w/w.[5] In other studies, the yields were set between 83,4 % a 87,97 % encapsulating essential oil of *Zanthoxylum limonella* by multiple emulsion and evaporation techniques.[27]

Likewise, the maximum efficiency observed was 96 %, at 45 and 60 min of crosslinking. These values could be the result of the fact that at greater amounts of time, crosslinking derives in a greater rigidness in the wall, and at the same time this reduces the retention of essential oil on the surface during the gelation.

Another study reports a lower Efficiency (88,6 %) at 6 min in the encapsulation of eucalyptus essential oil[28]

also observing a dependence on crosslinking time and independence at salt concentration of crosslinking. Cinnamon and thyme essential oil were also encapsulated observing similar encapsulation efficiency values (between 90 and 95 %) using calcium chloride concentrations at 0,5 % and a crosslinking time of 20 min.[29] The efficiencies found at encapsulating *Satureja hortensis* and *Rosmarinus officinalis* extracts were lower (4,79 % and 14,76 %).[8] Recent investigations have reported Efficiencies from 45 to 66 % when using ionic gelation for food when encapsulating marjoram essential oil.

The statistical analysis showed that the models for encapsulation efficiency and yield were appropriate, with a significant R^2 (0,792 and 0,786, respectively). Besides, it showed a p-value of lack of fit larger than 0,05, using a significance level of 5 % in both cases. The calcium chloride concentration has a linear significant effect on the yield and efficiency of microcapsules; as the ion Ca^{2+} concentration increases, the matrix crosslinking is facilitated. The time variable has a significant linear effect on efficiency, but not on yield. This could happen due to the transference of water, which is part of the emulsion (sodium-alginate solution at 1 % w/v) during crosslinking. At the same time, the time variable only influences in a quadratic way on the microencapsulation yield, and it is possible that some kind of interaction existed between these factors in the case of encapsulation efficiency.[4]

The encapsulation efficiency (E %) and yield (Y %) models obtained are shown in equations 5 and 6 in uncoded units. For a 2 % w/w GEO charge:

$$E\ \% = 84{,}96 + 0{,}383\ A + 0{,}358\ B + 0{,}0136\ AA - 0{,}003\ BB - 0{,}008\ AB \quad \textbf{(5)}$$

$$Y\ \% = 27{,}5 + 4{,}21\ A - 0{,}06\ B - 0{,}165\ AA - 0{,}000\ BB + 0{,}003\ AB \quad \textbf{(6)}$$

where A and B correspond to the concentration of calcium chloride and the time of the crosslinking process, respectively.

Efficiency and yield contour and response surface graphics (Figures 3 and 4) were generated from regression models. It could be observed that the maximum efficiencies (> 96 %) were obtained for C $CaCl_2$ between 9 and 10 % w/v between 40 and 60 min, the maximum being at 45 min, approximately. Likewise, the highest yields were obtained with crosslinking concentrations between 9 and 10 % w/v and, without the time variable affecting these results.

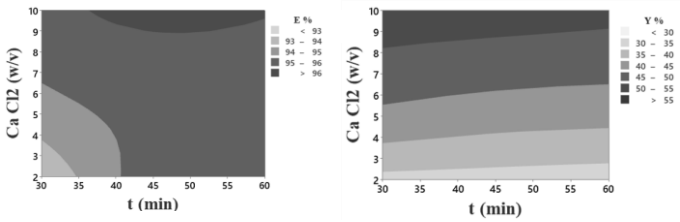

Figure 3- Contour Diagram of, a: % Efficiency and b: % Yield for microencapsulation with a load of 2 % w/w of GEO

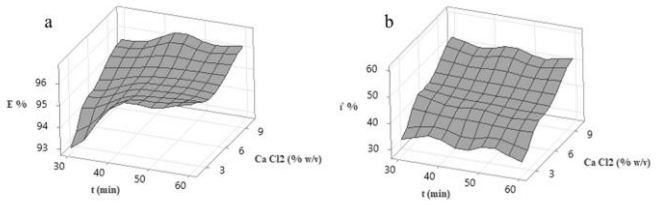

Figure 4- Surface Diagram of, a: % of Efficiency and b: % of yield for microencapsulation with a load of 2 % w/w of GEO

The total desirability, a function that evaluates the optimization when various responses are involved was 0,83, denoting that the configuration of both responses achieved favourable results in the maximization step. The individual desirability calculated indicates that the configurations are much more effective for maximizing the efficiency (d= 0,938) than for maximizing the yield (d= 0,73). According to the model, with a sodium chloride concentration at 10 % w/v and a crosslinking time of 46 min, a yield of 51,7 % and an Efficiency of 96,4 % would be obtained.

Five runs at the optimal point validated the model, achieving an efficiency of 96,03 ± 1,16 in percentage terms and a yield of 43,37 ± 3,22 in percentage terms demonstrating an adjustment to the model.

Crosslinking Kinetics and Kinetics Model

The crosslinking speed was studied in a calcium chloride solution at 10 % w/v (optimum value). The data are shown in Figure 5. The adjustment of empirical data was evaluated through the Elovich model obtaining an R^2 of 0,994. It could be observed that the adsorption rate curve follows an exponential trend and reached equilibrium at 15 min of crosslinking, and it showed at 2 min a slight movement to higher values of ion Ca^{2+} concentrations, due to the amount of ions in the medium.

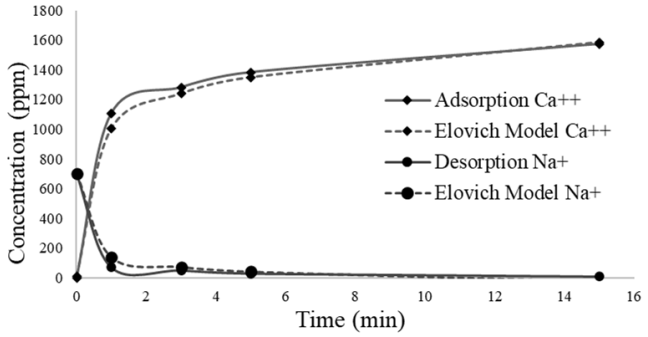

Figure 5- Adjustment of experimental data of Ca^{2+} adsorption with the Elovich model

The kinetic equations of adsorption and desorption of Elovich in calcium chloride, respectively obtained are the following (Equations 7 and 8).

$$q_{(t)a\ 10\ \%} = \frac{1}{4{,}576}\ln(23{,}293 * 4{,}576 * t) \quad (7)$$

$$q_{(t)d\ 10\ \%} = \frac{1}{-16{,}3931}\ln(0{,}0078 * 16{,}393 * t) \quad (8)$$

The value of the initial adsorption speed was 23,293 $g{\cdot}mg^{-1}{\cdot}min^{-1}$and might be due to the availability of Ca^{2+} in the crosslinking medium. The values of the constant term of adsorption (related to the covered surface and the activation energy by chemisorption) were 4,576 $g{\cdot}mg^{-1}$ for adsorption and -16,393 $g{\cdot}mg^{-1}$ for desorption. Although we could not find studies reporting the kinetics of Ca^{2+} adsorption in the crosslinking process, other works considered the adsorption speed of other metals over solid organic surfaces[21] that also fitted well the Elovich model. This model explains the processes of chemisorption and assumes that the active sites of sodium alginate are heterogeneous with different activation energies.[30]

It could be observed a fast chemisorption at the beginning due to the formation of dimers that create the egg-box of the calcium alginate and that after 5 min, it slowed down considerably due to a progressive and uniform introduction of Ca^{2+} as a result of the increase of the superficial crosslinking and the steady stirring. Simultaneously, the aggregation of the dimers led to the formation of an organized three-dimensional structure of bonds without heterogeneous grouping.[31] This could also explain the influence of the optimized crosslinking time on the efficiency of the encapsulation process. Longer crosslinking times would lead to a crosslinking network more organized and has a better packing of the three-dimensional egg-box minimizing the transfer of GEO to the surface of the microcapsule. This matches the study of controlled release considered below.

Microcapsules Characterization

The spectrum FTIR of the alginate-GEO microcapsules can be observed in Figure 6. It could be seen that in the microcapsule the spectrum copies the bands corresponding to sodium alginate which were previously described. It could also be seen that it copies the region of the GEO confirms their presence within the microcapsule and shows the compatibility of alginate as a carrier of natural bioactive components. Similar results have been obtained by other authors when performing encapsulation of GEO with sodium alginate[28,18] and other natural components such as the *Stevia rebaudiana* extract.[6]

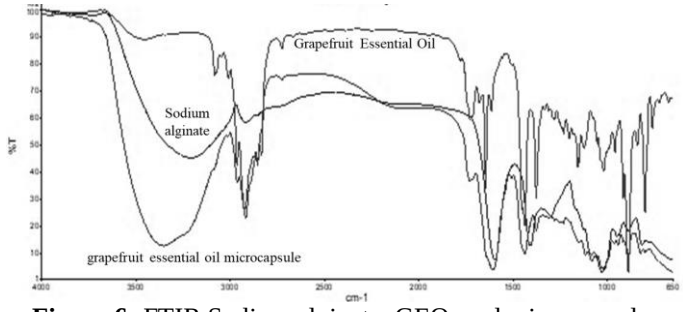

Figure 6- FTIR Sodium alginate, GEO, and microcapsules containing GEO

Obtaining Microcapsules with Modified Matrices

Average yield and encapsulation efficiency values, expressed as a percentage, for each treatment can be observed in Figure 7. It is noteworthy that efficiencies, in all cases, remained above 96 %. Additionally, both efficiency and yield were higher for matrices containing solids compared to those without solids, with the lignin-containing matrix exhibiting the best performance. This can be attributed to the GEO and water being retained within the pores of the solid. Other authors have also encapsulated active principles in modified matrices, such as guava leaf extract in alginate and starch, and although they did not report efficiency and yield values, they noted the retention of aroma in silicates due to entrapment in porous microregions.[32]

To select the best solids concentration in the matrix, a comparison of means, applying the Tukey method (α= 0,05), was conducted. The results are shown in Table 1.

A significant difference ($p < 0,05$) was observed solely in the yield of lignin microcapsules, which reached a maximum of 99,913 % efficiency and 67,183 % yield at a 1 % concentration (Table 1). While no significant differences were observed with silica, the silica matrix modification (0,8 %) achieved a maximum efficiency of 97,671 % with a corresponding yield of 52,306 %.

Microcapsules Characterization

Morphology and Size

The diameters of 50 microcapsules with alginate-GEO matrix were measured using data processing software. A mean value of 1,87 ± 0,31 mm was obtained. The measured diameters of the matrices modified with solids were between 1,75 and 2,00 mm.

Images of the microcapsules obtained with different matrices are observed in Figure 8a-c. In all cases, their spherical shape with a typical colour according to the matrix composition, can be seen.

The drying at 50 °C for an hour significantly reduced the size of the microcapsules (Figure 8d-f). A medium diameter of a dry particle of 0,6 ± 0,04 mm was obtained, and it was measured using an optical microscope with incorporated software.

Moisture content values before and after drying are presented in Table 2. The greatest water loss was observed in the alginate-GEO matrix, clearly indicating the ease with which water evaporates from this matrix without solids. However, the higher water retention observed in the matrices containing lignin and silica could be attributed to water retention within the pores of the solids.

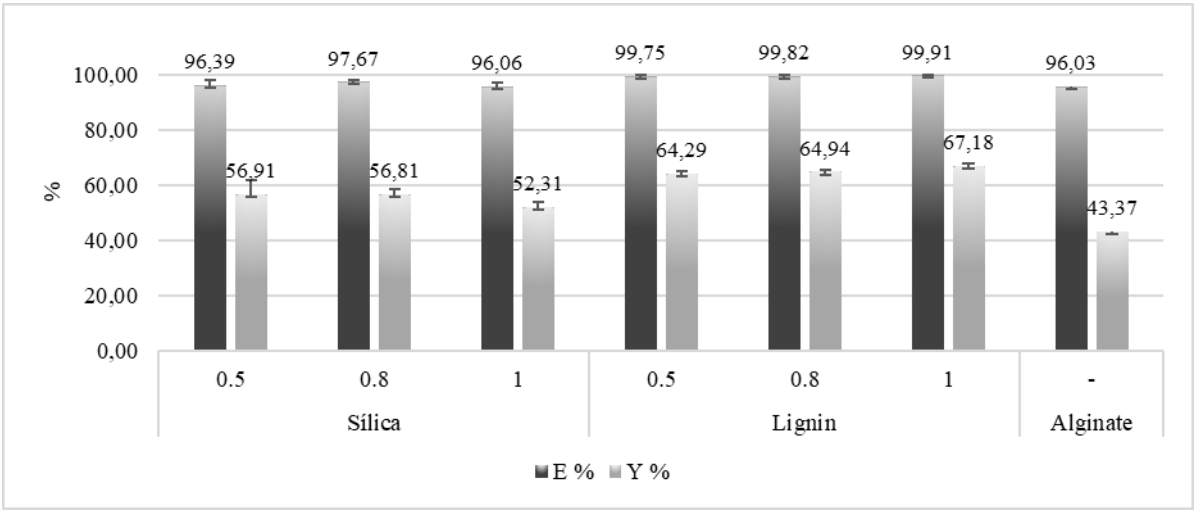

Figure 7- Values of microencapsulation Efficiency and Yield of grapefruit essential oil at 2 % w/w with different matrices containing alginate and modified matrices with lignin and silica

Table 1- Comparison of Tukey: yield (Y %) and efficiency (E %)

Solid	% w/w	Y%	Group*	P value Anova	E%	Group*	P value Anova
	0,5	64,293	B		99,755	A	
Lignin	0,8	64,937	B	0,000	99,824	A	0,386
	1,0	67,183	A		99,913	A	
	0,5	56,910	A		96,060	A	
silica	0,8	56,814	A	0,208	97,671	A	0,288
	1,0	52,306	A		96,385	A	

**The means that do not share a letter are significantly different.*

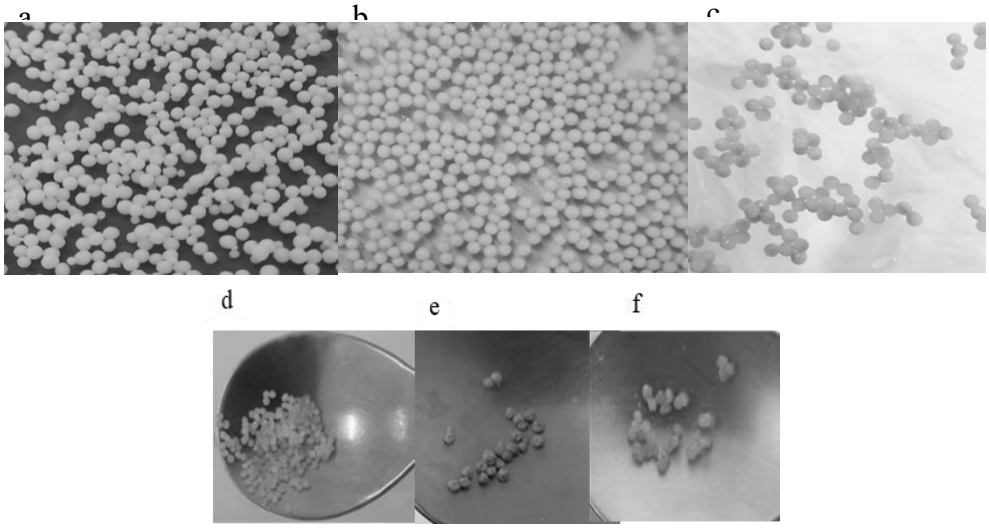

Figure 8- Images of the wet and dry microcapsules: a and d: alginate-GEO, b and e: alginate-silica-GEO; c and f: alginate-Lignin-GEO

Table 2- Moisture of microcapsules

Microcapsules-Matrix composition	**% solids**	**Moisture % wet microcapsules**	**Moisture % dry microcapsules**
GEO- Alginate-	-	87,4 ± 0,80	8,5 ± 1,4
GEO- Alginate-Silica	0,8	82,043 ± 1,064	27,4 ± 0,9
GEO- Alginate-Lignin	1	85,067 ± 0,275	51,1 ± 1,5

SEM images (Figure 9 a-c) with different magnifications show that the surfaces of the microcapsules are porous like a sponge, which indicates the sodium alginate crosslinking. Similar results were obtained by Soliman *et al.* in the encapsulation of clove and thyme essential oil[29] and with the results obtained by Leal Mazza *et al.* in the encapsulation of marjoram essential oil.[4]

It could be observed that the solid did not interfere in the alginate crosslinking; the surface of the microcapsules with solid (b and c) presented a similar morphology (lumpy, wave-shaped) of the matrix without solid (a) This could be due to the presence of GEO droplets on the exterior or interior surface of the microcapsules which could cause these lumps. The shrinking of the cell wall occurred due to the lyophilization process the microcapsule went through before being analyzed by electronic microscopy. Similar results were obtained by other authors, although their studies consisted of alginate matrices with other components such as whey protein to encapsulate marjoram oil,[4] or to encapsulate other components such as bacteria in alginate matrix with starch,[33] or to absorb metals in an alginate matrix with silica.[34] At the same time, it could be observed a higher amount of pores on the surface of the microcapsule with lignin and silica, which could be due to the presence of these solids in the matrix.

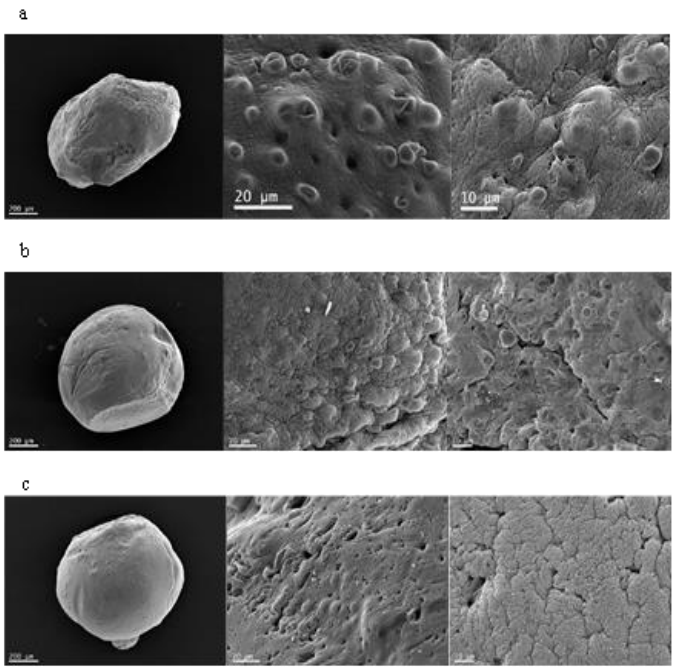

Figure 9- SEM images of microcapsules of a: Aginate- GEO, b: Alginate-Silica-GEO; c: Alginate- Lignin-GEO, with increases of 75x, 700x and 1000x, respectively

Controlled Release

The controlled release of GEO was analyzed in an alcoholic medium (isopropyl alcohol) to facilitate its solubility. The profiles of the releases related to each matrix in a wet or dried state can be seen in Figure 10. In all the cases, two phases could be observed: one

with an initial faster release or an initial “burst” and, a slower one afterward.[35] The first phase of the release could be attributed to a purely diffusional stage as a consequence of the volume expansion of the polymer due to the relaxation of its chains when submerged in liquids and to the GEO available on the surface of the microcapsule.[8] Besides, wet matrix microcapsules showed a slower initial release rate than dry microcapsules. This can be attributed to the greater accessibility of GEO when the microcapsule had a lower water content and to the presence of GEO on the surface after drying.[36] Furthermore, in matrices containing lignin and silica, the initial release rate was significantly higher compared to matrices without solid particles. This phenomenon can be attributed to the increased availability of GEO within the solid particles near the matrix surface at the start of the liberation.

As regards the release percentage, it could be observed that for up to 210 min the alginate matrices reached 85 % of GEO release, and the matrices modified with solids reached, approximately, 80 % of release. Besides, the matrices without modification released more than 90 % during the first 24 h; whereas the ones that had silica continued releasing for 7 days reaching 95-98 % (data not shown) Only the matrices with lignin, whose release rate after 7 days was of 83 %, continued for 15 days completing the 98 %. This delayed release observed in matrices with solids could be due to the content of GEO in the internal pores of the solids and also due to the presence of solid particles in regions furthest from the matrix surface.[3] Besides, other authors have encapsulated hydrophobic molecules in a lignin matrix chemically modified reaching a release of 60 % in 36 h.[3] In another study it was reported that a complex matrix was made, which was composed of nanoparticles of silica, chitosan, and hydroxypropyl cellulose to encapsulate mint essential oil, achieving a delayed release of the GEO of more than 15 days, but in a non-alcoholic medium, which explains the delay due to physisorption of the essential oil over the solid.[37]

The release rates obtained are faster than the ones reported in other studies (60 to 78 % in 9 h with 1 at 3 % v/v of GEO load), but in an aqueous medium where the GEO is not soluble. The slower release at the end is typically linked to particle size, larger sizes exhibiting lower release rates due to a decreased surface-to-volume ratio,[3] as is the case with wet particles.[8]

The GEO release mechanism from different matrices was studied by fitting the release profiles to various models, as shown in Table 3. A successful fit of the solid-free treatments to the Peppas model was obtained in the first part of the release (up to 60 % of GEO). The exponent of the Peppas model for the Wet alginate-GEO treatment indicates an "anomalous" transport, characterized by a superposition of various phenomena, including drug diffusion and polymer swelling.[38] In contrast, for the dry alginate-GEO treatment, the release exponent indicates a mechanism that combines partial diffusion through a swollen matrix and through water-filled pores.

On the other hand, treatments with solids, both dry and wet, show a successful fit to the empirical Weibull equation, demonstrating the value of its parameters (Table 4) which have an abrupt initial release, or "burst effect".[28] Moreover, previous studies have shown that the Weibull model provides an excellent fit for the entire release curve when the release mechanism is governed by Fickian diffusion.[39] There is no previous work reporting the diffusional exponent under similar conditions of matrices, encapsulated active ingredient, and release medium.

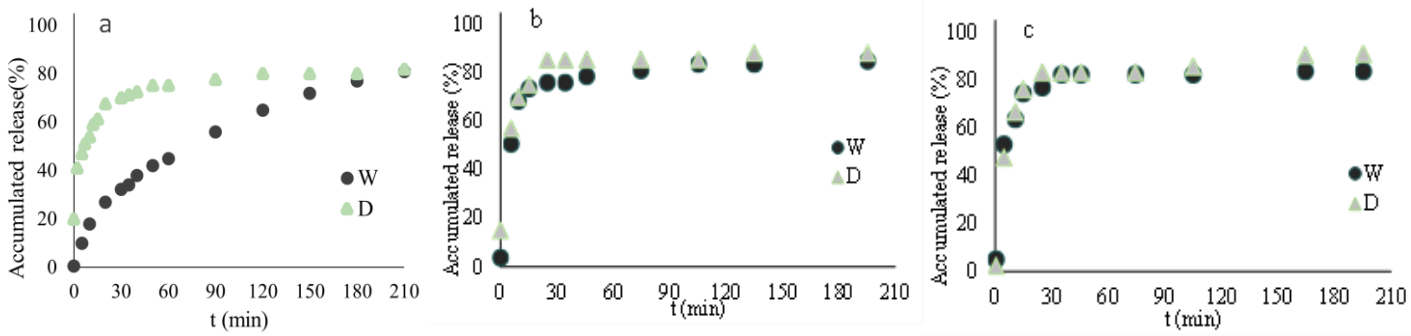

Figure 10- Diagrams of controlled release of GEO, a: Alginate-GEO; b: Alginate-lignin-GEO; c: Alginate-silica-GEO

Table 3- R^2 coefficients of the mathematical models

Treatment	Peppas and Korsmeyer	Weibull	Orden 0	Higuchi
wet Alginate-GEO	0,997 0	0,990 3	0,895 1	0,997 7
wet Alginate-lignin-GEO	-	0,954 1	0,309 1	0,604 7
wet Alginate-silica-GEO	-	0,946 0	0,375 7	0,555 6
dry Alginate- GEO	0,971 0	0,953 9	0,384 2	0,953 9
dry Alginate-Lignin- GEO	-	0,963 2	0,304 1	0,539 2
dry Alginate-Silica- GEO	-	0,947 0	0,284 0	0,508 6

Table 4- Parameters of mathematical models

Peppas and Korsmeyer	Weibull			
Treatment	**k**	**n**	**a**	**b**
wet Alginate-GEO	1,670	0,523 0	0,187 7	0,236 8
wet Alginate-lignin-GEO	-	-	0,104 5	0,465 3
wet Alginate-silica-GEO	-	-	0,100 6	0,478 1
dry Alginate-GEO	3,734	0,110 6	0,031 3	0,575 5
dry Alginate-lignin-GEO	-	-	0,045 2	0,568 2
dry Alginate-silica-GEO	-	-	0,211 0	0,306 4

CONCLUSIONS

The active compound employed was grapefruit essential oil, produced by a local citrus company. The microencapsulation of GEO with sodium alginate, through external ionic gelation and extrusion, was optimized with a 2 % w/w GEO loading. The validation of the optimal process was evaluated through the desirability function, resulting in an average efficiency of 96,03 ± 1,16 % and an average yield of 43,37 ± 3,22 %. The adsorption and desorption of Ca^{2+} in the crosslinking process were shown to fit the Elovich model. Additionally, the addition of lignin and silica (both obtained from rice husk biomass) to the microcapsule matrix improved yields and efficiencies. In this way, the properties of the added components were exploited, and the economic value of the biomass components was increased. The controlled release profiles of the obtained microcapsules were fitted to the Weibull model. Matrices without solids successfully fitted the Peppas and Korsmeyer model for polymeric systems. Furthermore, vacuum drying reduced the moisture content of the microcapsules, as well as their diameter. This improved handling and increased their potential applications in food preservation, cosmetics, and pharmaceuticals. The methodology employed was simple and did not involve hazardous solvents or components that could harm the environment.

ACKNOWLEDGMENT

The authors thank the Mager company from the province of Corrientes, Argentina, for providing the essential grapefruit oil, and they acknowledge financial support from the National Technological University for this research work.

REFERENCES

1. TABAN, A.; SAHARKHIZ, M. J.; HOOSHMANDI, M. “Insecticidal and repellent activity of three Satureja species against adult red flour beetles, Tribolium castaneum (Coleoptera: Tenebrionidae)” En línea. *Acta Ecologica Sinica.* 2017, **37**(3), 201-206. http://dx.doi.org/10.1016/j.chnaes.2017.01.001

2. RIOS MERA, J. D. *et al*. “Encapsulation optimization and pH- and temperature-stability of the complex coacervation between soy protein isolate and inulin entrapping fish oil”. *LWT*. 2019, **116,** 108555. https://doi.org/10.1016/j.lwt.2019.108555

3. CHE, N.; DEMPERE, L. A.; TONG, Z. “Synthesis of pH-Responsive Lignin-Based Nanocapsules for Controlled Release of Hydrophobic Molecules”. *ACS Sustainable Chemistry & Engineering*. 2016, **4**(10), 5204-5211. https://doi.org/10.1021/acssuschemeng.6b01209

4. LEAL MAZZA, K. *et al*. “Microencapsulation of marjoram essential oil as a food additive using sodium

alginate and whey protein isolate". *International Journal of Biological Macromolecules.* 2023, 123478. https://doi.org/10.1016/j.ijbiomac.2023.123478
5. BENAVIDES, S.; CORTÉS, P.; PARADA, J.; FRANCO, W. "Development of alginate microspheres containing thyme essential oil using ionic gelation". *Food chemistry*. 2016, **204**, 77-83. http://dx.doi.org/10.1016/j.foodchem.2016.02.104
6. ARRIOLA, N. D. *et al*. "Encapsulation of stevia rebaudiana Bertoni aqueous crude extracts by ionic gelation - Effects of alginate blends and gelling solutions on the polyphenolic profile". *Food Chemistry*. 2019, **275**, 123-134. https://doi.org/10.1016/j.foodchem.2018.09.086
7. DA SILVA C., A. G. *et al*. "Anthocyanins from jussara (*Euterpe edulis Martius*) extract carried by calcium alginate beads pre-prepared using ionic gelation". *Powder Technology.* 2019**,** **345**, 283-291. https://doi.org/10.1016/j.powtec.2019.01.016
8. POPESCU, L. *et al*. "The Effect of Aromatic Plant Extracts Encapsulated in Alginate on the Bioactivity, Textural Characteristics and Shelf Life of Yogurt". *Antioxidants*. 2023, **12**(4), 893. https://doi.org/10.3390/antiox12040893
9. ATENCIO, S.; MAESTRO, A.; SANTAMARIA, E.; GUTIÉRREZ, J. M.; GONZÁLEZ, C. "Encapsulation of ginger oil in alginate-based shell materials". *Food Bioscience*. 2020, **37**, 100714. https://doi.org/10.1016/j.fbio.2020.100714
10. BELSCAK CVITANOVIC, A. *et al.* "Emulsion templated microencapsulation of dandelion (Taraxacum officinale L.) polyphenols and β-carotene by ionotropic gelation of alginate and pectin". *Food hydrocolloids*. 2016**,** **57**, 139. http://dx.doi.org/10.1016/j.foodhyd.2016.01.020
11. SAIFULLAH, M.; SHISHIR, M. R. I.; FERDOWSI, R.; RAHMAN, M. R. T.; VAN VUONG, Q. "Micro and nanoencapsulation, retention and controlled release of flavor and aroma compounds: A critical review". *Trends in Food Science & Technology*. 2019, **86**, 230-251. https://doi.org/10.1016/j.tifs.2019.02.030
12. CHAN, E. S. "Preparation of Ca-alginate beads containing high oil content: Influence of process variables on encapsulation efficiency and bead properties". *Carbohydrate Polymers.* 2011, **84**(4), 1267-1275. https://doi.org/10.1016/j.carbpol.2011.01.015
13. LI, M.; JIANG, X.; WANG, D.; XU, Z.; YANG, M. "*In situ* reduction of silver nanoparticles in the lignin-based hydrogel for enhanced antibacterial application". *Colloids and Surfaces B: Biointerfaces.* 2019**,** **177**, 370-376. https://doi.org/10.1016/j.colsurfb.2019.02.029
14. HAN, X.; LIANG, J.; FUKUDA, S.; ZHU, L.; WANG, S. "Sodium alginate-silica composite aerogels from rice husk ash for efficient absorption of organic pollutants. Biomass and Bioenergy" *Biomass and Bioenergy.* 2022, **159**, 106424. https://doi.org/10.1016/j.biombioe.2022.106424
15. VASEK, O. M.; CÁCERES, L. M.; CHAMORRO, E.; VELASCO, G. A. "Antibacterial activity of Citrus paradisi essential oil". *Journal of Natural Products.* 2015, **8**, 16-26. http://hdl.handle.net/20.500.12272/941
16. CÁCERES, L. M.; VELASCO, G. A.; DAGNINO, E. P.; CHAMORRO, E. R. "Microencapsulación de Aceite de Pomelo con Alginato de Sodio por Gelificación y Extrusión Iónica: Optimización y Modelado de la Reticulación y Estudio de la Cinética de Liberación Controlada". *Revista Tecnología y Ciencia.* 2020, **39**, 41-61. https://doi.org/10.33414/rtyc.39.41-61.2020
17. DAGNINO, E. P.; CHAMORRO, E. R.; ROMANO, S. D.; FELISSIA, F. E.; AREA, M. C. "Optimization of the acid pretreatment of rice hulls to obtain fermentable sugars for bioethanol production". *Industrial Crops and Products.* 2013**,** **42**, 363. https://doi.org/10.1016/j.indcrop.2012.06.019
18. LEVIĆ, S. *et al*. "Characterization of sodium alginate/d-limonene emulsions and respective calcium alginate/d-limonene beads produced by electrostatic extrusion". *Food Hydrocolloids.* 2015, **45**, 111-123. https://doi.org/10.1016/j.foodhyd.2014.10.001
19. MONTGOMERY, D. C. *Diseño y análisis de experimentos*. 2ª Edición. México: Limusa Wiley, 2003**.** 686 p. ISBN: 9681861566.
20. MAJI, T. K.; BARUAH, I.; DUBE, S.; HUSSAIN, M. R. "Microencapsulation of Zanthoxylum limonella oil (ZLO) in glutaraldehyde crosslinked gelatin for mosquito repellent application". *Bioresource Technology.* 2007, **98**(4), 840-844. https://doi.org/10.1016/j.biortech.2006.03.005
21. TANG, S. *et al*. "Construction of physically crosslinked chitosan/sodium alginate/calcium ion double-network hydrogel and its application to heavy metal ions removal". *Chemical Engineering Journal.* 2020, **393**, 124728, https://doi.org/10.1016/j.cej.2020.124728
22. DERDAR, H.; BELBACHIR, M.; HARRANE, A. "A Green Synthesis of Polylimonene Using Maghnite-H+, an Exchanged Montmorillonite Clay, as Eco-Catalyst". *Bulletin of Chemical Reactions*

Engineering & Catalysis. 2019**,** **14**(1), 69-78. https://doi.org/10.9767/bcrec.14.1.2692.69-78
23. VAN HOOGMOED, C. G.; BUSSCHER, H. J.; DE VOS, P. "Fourier transform infrared spectroscopy studies of alginate-PLL capsules with varying compositions". *Journal of Biomedical Materials Research A.* 2003**,** **67**(1),172-178. https://doi.org/10.1002/jbm.a.10086
24. UM, H.; KANG, R. H.; KIM, D. "Iron-silicate-coated porous silicon nanoparticles for in situ ROS self-generation". *Colloids and Surfaces B: Biointerfaces* . 2023, **225** 113273. https://doi.org/10.1016/j.colsurfb.2023.113273
25. CAREY, F. A. *Química Orgánica.* 6ª Edición. México: McGraw-Hill Interamericana, 2014. 1424 p. ISBN: 970-10-5610-8
26. ONAIZI, S. A. *et al*. "Crude oil/water nanoemulsions stabilized by biosurfactant: Stability and pH-Switchability". *Journal of Petroleum Science and Engineering*. 2021, **198**, 108173. https://doi.org/10.1016/j.petrol.2020.108173
27. BANERJEE, S. *et al.* "Influence of process variables on essential oil microcapsule properties by carbohydrate polymer-protein blends". *Carbohydrate Polymers.* 2013, **93**(2), 691-697. https://doi.org/10.1016/j.carbpol.2013.01.028
28. NOPPAKUNDILOGRAT, S.; PIBOON, P.; GRAISUWAN, W.; NUISIN, R.; KIATKAMJORNWONG, S. "Encapsulated eucalyptus oil in ionically cross-linked alginate microcapsules and its controlled release". *Carbohydrate Polymers.* 2015, **131**, 23-33. https://doi.org/10.1016/j.carbpol.2015.05.054
29. SOLIMAN, E. A.; EL MOGHAZY, A. Y.; MOHY EL-DIN, M. S.; MASSOUD, M. A. "Microencapsulation of Essential Oils within Alginate: Formulation and *in vitro* Evaluation of Antifungal Activity". *Journal of Encapsulation and Adsorption Sciences.* 2013, **3**(01), 48-55. http://dx.doi.org/10.4236/jeas.2013.31006
30. SHAMSUDIN, M. S. *et al*. "Performance and interactions of diclofenac adsorption using Alginate/Carbon-based Films: Experimental investigation and statistical physics modelling". *Chemical Engineering Journal.* 2022, ***428***, 131929. https://doi.org/10.1016/j.cej.2021.131929
31. FARRÉS, I. F.; NORTON, I. T. "Formation kinetics and rheology of alginate fluid gels produced by *in situ* calcium release". *Food Hydrocolloids.* 2014, **40**, 76-84. http://dx.doi.org/10.1016/j.foodhyd.2014.02.005
32. ASHRAF, M. A.; KHAN, A. M.; AHMAD, M.; SARFRAZ, M. "Effectiveness of silica based sol-gel microencapsulation method for odorants and flavors leading to sustainable environment". *Frontiers in Chemistry.* 2015, **3**, 42. https://doi.org/10.3389/fchem.2015.00042
33. MARTIN, M. J.; LARA VILLOSLADA, F.; RUIZ, M. A.; MORALES, M. E. "Effect of unmodified starch on viability of alginate-encapsulated Lactobacillus fermentum CECT5716". *LWT - Food Science and Technology.* 2013, **53**(2), 480-486. https://doi.org/10.1016/j.lwt.2013.03.019
34. SHIM, J.; LIM, J. M.; SHEA, P. J.; OH, B. T. "Simultaneous removal of phenol, Cu and Cd from water with corn cob silica-alginate beads". *Journal of Hazardous Materials.* 2014**,** **2,** 129-136. https://doi.org/10.1016/j.jhazmat.2014.03.010
35. SIEPMANN, J.; FAISANT, N.; BENOIT, J. P. "A New Mathematical Model Quantifying Drug Release from Bioerodible Microparticles Using Monte Carlo Simulations". *Pharmaceutical Research*. 2002, **19**(12), 1885-1893. ISSN: 1573-904X. https://doi.org/10.1023/A:1021457911533
36. LOCALI PEREIRA, A. R.; LOPES, N. A.; MENIS HENRIQUE, M. E. C.; JANZANTTI, N. S.; NICOLETTI, V. R. "Modulation of volatile release and antimicrobial properties of pink pepper essential oil by microencapsulation in single- and double-layer structured matrices". *International Journal of Food Microbiology*. 2020, **335**, 108890. https://doi.org/10.1016/j.ijfoodmicro.2020.108890
37. LAI, H. *et al.* "Fabrication and antibacterial evaluation of peppermint oil-loaded composite microcapsules by chitosan-decorated silica nanoparticles stabilized Pickering emulsion templating". *International Journal of Biological Macromolecules.* 2021, **183**, 2314. https://doi.org/10.1016/j.ijbiomac.2021.05.198
38. FERNÁNDEZ, J. A.; SANTOS, R. G.; ESTÉVEZ, G. F. "Cinética de liberación de cefalexiana desde un biomaterial compuesto por HAP-200/POVIAC/CaCO3". *Anales de la Real Academia Nacional de Farmacia.* 2009, **75**(3). https://core.ac.uk/download/pdf/230310909.pdf
39. PAPADOPOULOU, V.; KOSMIDIS, K.; VLACHOU, M.; MACHERAS, P. "On the use of the Weibull function for the discernment of drug release mechanisms". *International Journal of Pharmaceutics,* 2006. **309**(1-2), 44-50. https://doi.org/10.1016/j.ijpharm.2005.10.044

INTEREST CONFLICT

The authors express that there are no conflicts of interest in the submitted manuscript.

AUTHOR'S CONTRIBUTION

Liliana M. Cáceres: conceptualization, methodology, formal analysis, writing-original draft preparation, visualization, investigation. Active participation in the discussion of the results.

Eliana P. Dagnino: supervision and review the manuscript critically for important intellectual content. Active participation in the discussion of the results.

Ester Chamorro: supervision and approval of the version of the manuscript to be published. Active participation in the discussion of the results.